01 Sep 2005

Charge-Exchange-Produced K -shell X-Ray Emission from Ar^{16+} in a Tokamak Plasma with Neutral-Beam Injection

P. Beiersdorfer

M. Bitter

M. Marion

Ronald E. Olson
Missouri University of Science and Technology, olson@mst.edu

Recommended Citation

P. Beiersdorfer et al., "Charge-Exchange-Produced K -shell X-Ray Emission from Ar^{16+} in a Tokamak Plasma with Neutral-Beam Injection," *Physical Review A*, American Physical Society (APS), Sep 2005. The definitive version is available at https://doi.org/10.1103/PhysRevA.72.032725

Channel electron multiplier and channelplate efficiencies for detecting positive ions

M. Krems, J. Zirbel, M. Thomason, and R. D. DuBois[a)]
Department of Physics, University of Missouri-Rolla, Rolla, Missouri 65409

(Received 7 April 2005; accepted 14 August 2005; published online 16 September 2005)

Absolute detection efficiencies for singly and multiply charged positive ions have been measured for a channelplate and for two different channel electron multipliers (CEM). The efficiencies were measured for impact energies between approximately 0.25 and 25 keV and for ion masses ranging from 14 to 132. The maximum efficiencies were found to be the same for all ions investigated and were approximately 58% for a channelplate and 89% for the CEMs. For a channelplate it is shown that the detection efficiencies for heavier ions scale to a single curve if plotted versus the impact energy divided by the square root of the ion mass. Data taken from the literature imply that lighter ions scale differently. Polynomial fitting parameters to the present efficiency curves are provided. © *2005 American Institute of Physics.* [DOI: 10.1063/1.2052052]

I. INTRODUCTION

For several decades channel electron multipliers (CEMs) and microchannelplate assemblies [channelplates (CPs)] have been the detectors of choice in many areas of basic and applied research. This is because of their high gains, low background signal rates and, as compared to discrete dynode detectors, stability over long time periods, especially in oxidizing environments. One particular widespread use is for the detection of low-energy ions. For example, in the area of atomic physics low-energy ions have been used to provide information about atomic and molecular ionization rates, about the number of electrons removed in single interactions, as well as information about breakup channels and fragmentation dynamics of simple molecules. In the field of material science, measurements of low-energy ions ejected from various materials are used to analyze surface and subsurface constituents and structure plus can provide information about erosion of surfaces due to photon or charged particle impact. Chemistry and biological uses include measuring ion products to study reaction channels and rates, or to analyze complex chemical and biological samples. Low-energy ion beams are often used as probes for the studies listed above and in these cases, postcollision beam ions are sometimes detected in order to obtain more detailed information or to isolate reaction channels or specific events.

Whatever the objective or field, all of these studies have one thing in common, namely the information is extracted by detecting low-energy target or beam ions. Since target ions are produced with kinetic energies ranging from milli- to a few-electron volts or when subkilo-electron volts ion beams are used, the detection efficiencies would be negligibly small. Therefore, to enhance their detection efficiencies the ions are accelerated to several kilo-electron volts (keV) energies by biasing the front of the detector. As a result, a critical factor in all of these studies is knowledge about CEM and CP detection efficiencies for different ion species having kinetic energies in the keV range.

However, even after decades of use there is limited information in the literature about absolute ion detection efficiencies for CEMs and channelplates. Of the studies previously performed,[1–15] all except three[6,7,15] reported efficiencies only for singly charged ions and roughly half of the studies only provided information for a single ion species or ion energy. The majority of the studies investigated channelplate arrays while four[1,6,11,12] measured efficiencies for CEMs. No study compared the two types of detectors.

To briefly summarize the earlier results, for channelplates the studies showed that the detection efficiencies decreased at lower impact energies but for energies around 3–5 keV tended to saturate at a value near that of the open aperture ratio of the plates. The falloff and saturation are in accordance with general expectations since the detected signal results from an electron avalanche initiated by secondary electrons liberated when the ion impacts the surface. When the energy is sufficiently high all projectiles impacting within or near an open channel should be detected with equal probability since any impact is capable of liberating secondary electrons and generating an electron avalanche. Therefore the maximum efficiency is limited by the open area of the detector. At lower energies according to the work of Parilis and Kishinevskii,[16] different ions have different threshold velocities below which no secondary electrons are emitted. Above the threshold energy their work predicts that the secondary emission probability increases with increasing impact velocity and the rate of increase depends on the ion species. Hence, the efficiencies are expected to increase with increasing impact energy or velocity and then saturate at a value that is limited by the open aperture ratio, i.e., by the sensitive area of the detector. As noted later, electric fields applied to suppress the loss of secondary electrons may influence the

a)Electronic mail: dubois@umr.edu

detection efficiency. The reader is also referred to the theoretical work of Fraser[17] who modeled the detection efficiencies for various positive ions.

In existing studies, maximum efficiencies corresponding to values near the open aperture ratio were seen except for one case[3] where Mg^+ ions were investigated. Here, the measured efficiencies exceeded the open aperture ratio and were continuing to increase at the highest energy investigated. Deconihout *et al.*[18] showed that detection efficiencies varied with the strength of the electric field used to repel secondary electrons back toward the surface of the channelplate and could exceed the open aperture ratio but their study used a phosphor anode. In their work, if a single impacting particle generated two secondary electrons and these electrons generated avalanches down different channels, these could be detected as separate events, unlike the case where charge amplification electronics are used where these would be counted as a single event.

Thus, the question that still arises is whether one can simply use the open aperture ratio for the maximum efficiency and, if so, what must the ion energy or velocity be in order to do this. Another open question is how to extrapolate beyond the ions or energies for which data are provided. Likely possibilities are that the detection efficiency depends upon the particle's energy or its velocity. This is particularly important at lower energies since existing data provide conflicting results as to whether the efficiencies depend on the impact energy or velocity or neither.

To address these questions, we have measured absolute efficiencies for detecting various singly and multiply charged positive ions. The data presented here cover an ion energy range between 0.25 and approximately 25 keV and ion masses ranging from 14 to 132 amu. For several species, different charge state ions were used. Efficiencies were measured for two CEMs, a recently purchased Burle Electronics CEM, model 4860, (CEM 1) and one purchased from Mullard approximately 20 years ago (CEM 2). The Mullard CEM, model unknown, is considered representative of an "aged" detector as it had been used in various atomic physics studies over a period of years while the Burle CEM is considered representative of "today's technology" and a new detector. For comparison, efficiencies were also measured for a channelplate array. For this, a newly purchased Burle channelplate, model 51003, was used. As will be shown, except for low-energy ion detection by CEMs, our present work yields very similar detection efficiencies for different CEM or CP detectors produced by different manufacturers. Therefore, within the accuracy of our measurements, detailed information such as specific model numbers, pore size, or bias angles are not considered to be major factors with regard to the absolute detection efficiencies and, hence, are not provided.

II. EXPERIMENTAL METHOD AND PROCEDURES

The apparatus consisted of a "standard" atomic physics recoil ion setup where an electron beam of approximately 1 keV was passed through a target cell and used to ionize various atomic and molecular gases. See Fig. 1. The target

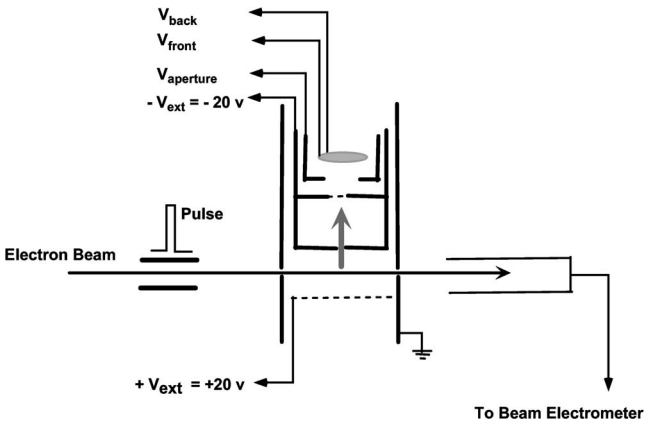

FIG. 1. Schematic of apparatus used to measure low-energy ion detection efficiencies. The vertical arrow depicts recoil ions extracted from the target region which pass though a field free region before impacting on a CEM or a CP detector.

ions were extracted by a transverse electric field ($\sim$80 V/cm) followed by a field free region after which they impacted the detector. The number of recoil ions was measured using both a "pulse counting" and an "ion current" mode. For both cases, an electrometer, voltage controlled oscillator, and scaler were used to integrate the electron beam exiting the target cell and a capacitance manometer was used to measure the absolute target pressure. By comparing the number of ions counted per incident electron and unit target density with the number calculated from the ion current, detection efficiencies were determined. In the following, unprimed symbols are used when referring to the number of ions counted (where the detection efficiency is less than unity) and primed symbols when referring to the actual number of ions impacting the detector as determined from the measured current.

In the "counting" mode, standard electronics were used to amplify, discriminate, and count the ion signal. Care was taken in setting the detector gain and discriminator such that all amplified signals were counted. The voltages applied to the front and back of the detector were such that the detector gain was held constant while varying the front voltage between 0.25 and 5 kV. In order to avoid loss of secondary electrons due to the strong attractive field between the detector and the exit of the ion time-of-flight tube, a biased aperture (for the CEM measurements) and a biased grid (for the CP measurements) were placed a couple millimeters in front of the detectors. This aperture/grid was biased approximately 25 V negative with respect to the detector front.

In the "current" mode, the electron beam current was increased from tens of picoamperes (pA) to a few tenths of a microamp; this increased the recoil ion signal to the tens of pA range. The counting electronics were disconnected and a second electrometer, voltage controlled oscillator, and scaler system were used to record and integrate the ion current reaching the detector. Care was taken that the detector and surroundings were biased such that all extracted ions were collected and that no secondary electrons produced by the incoming ion flux were lost, plus any electron current from the scattered beam was negligible. Typical voltages for this were; voltage applied to extract the ions, −20 V; aperture/

grid voltage, −35 V; detector voltage, −28 V. Last, conversion of the integrated ion and electron currents to number of particles was checked using a calibrated current source.

For each target gas, the efficiency measurements consisted of three steps. The first step was comprised of ion time-of-flight (TOF) measurements. This provided information about the relative number of recoil ions detected for each charge state at various impact energies plus whether any residual gas contamination needed to be taken into account in the efficiency calculation. These measurements consisted of adjusting the electron beam intensity and target pressure such that the target ion count rate was approximately 15–20 kHz. Then the electron beam was pulsed by applying a fixed voltage to one plate of the beam steering deflectors, see Fig. 1, and a short (100–150 ns) pulse to the other plate. Using the recoil ion signal and the delayed beam pulse as START-STOP coincidence signals, TOF spectrum were collected for various impact energies. For this, the voltage at the front of the detector was varied while maintaining a constant voltage difference between the front and rear of the detector. From these data, charge state fractions, $F_q(V_{\text{front}})=N_q/\Sigma N_q$, were calculated as a function of the front bias voltage V_{front}. Here N_q is the background subtracted intensity for a particular charge state. Typically spectra were collected until the statistical uncertainties for the most intense charge states were all less than 5%.

As it was difficult to accurately integrate the small electron beam currents and maintain a constant gas pressure over the long time needed to accumulate the TOF spectra, the next step was to quickly count the total number of ions detected, N_{tot}, at each value of V_{front} while maintaining a constant target pressure and integrating the electron beam current. This was done by removing the pulse voltage and integrating the recoil ion counts and electron beam currents for 10–20 s at each bias voltage. Then the target gas was removed and background intensities were measured and subtracted.

From these two steps the relative number of ions for each charge state per unit target pressure and incident electron was determined as a function of the impact energy using the following equation:

$$N_q(E_q) = F_q(\mathrm{V}_{\text{front}})N_{\text{tot}}(V_{\text{front}}). \tag{1}$$

Here the kinetic energy E_q for each charge state is given by qV_{front}, values for $F_q(V_{\text{front}})$ are obtained from the TOF measurements (step 1 earlier), and values for $N_{\text{tot}}(V_{\text{front}})$ are taken from the step 2 measurements.

Plotting $N_q(E_q)$ vs E_q demonstrated that all the charge state ions had similar shapes and, except for the heaviest singly charged ions, the curves for different charge states reached a constant value at the highest impact energies investigated. Therefore, all the curves were normalized to the same value at high energies, i.e., in the energy range where N_q reached a constant value. Except for small modifications, the normalization factor is $1/F_q(\infty)$, where ∞ means that the fractions used are average values taken for large values of V_{front} where F_q was found to reach a constant value. By this method, a single curve for the relative counts versus the impact energy was generated; this curve being equivalent to the relative detection efficiency as a function of impact energy.

The final step was to place these relative curves on an absolute scale. This was done by measuring and comparing the total number of ions counted with the total number calculated from the measured ion current, each being measured per incident electron and as a function of target pressure. In the counting mode, the detector was biased at the highest value possible, typically at 4.5 or 5 kV, and the ratio of the number of recoil ions counted per incident electron was called R_c. In the current mode, as previously stated the detector bias voltages and preamplifier were replaced by an electrometer attached to the detector and the bias voltages were changed. Here, the ratio of the recoil ion current with respect to the incident beam current is referred to as R_I.

In the counting mode, R_c is proportional to the total number of ions counted, N_{counted}, which is equal to the sum of the number of ions for each charge state that impact the detector, N'_q, times the detection efficiency at the particular energy for each charge state, $\eta_q(qV_{\text{front}})$. Hence,

$$N_{\text{counted}} = \sum_q \eta_q(qV_{\text{front}})N'_q. \tag{2}$$

As previously stated, our relative counts versus impact energy are equivalent to the relative detection efficiency as a function of impact energy. Thus, the ratio of the number of counts at a certain energy qV_{front} with respect to those at a very high energy ∞ is the same as the ratio of the efficiencies at these two points, i.e., $\eta_q(qV_{\text{front}})/\eta(\infty)=N(qV_{\text{front}})/N(\infty) \equiv k_q(qV_{\text{front}})$. Hence, in Eq. (2), $\eta_q(qV_{\text{front}})$ can be replaced by $\eta(\infty)k_q(qV_{\text{front}})$ where $k_q(qV_{\text{front}})$ is the number of scaled counts at energy qV_{front} divided by the number of scaled counts at the highest energies we measured. Note that the subscript q indicates that the value of k is different for each charge state because different charge states impact with different energies. In addition, $N'_q=F_q(\infty)N'_{\text{tot}}$ where these quantities have been defined earlier. Thus, Eq. (2) can be rewritten as

$$\begin{aligned} N_{\text{counted}} &= \sum_q \eta(\infty)k_q(qV_{\text{front}})F_q(\infty)N'_{\text{tot}} \\ &= \eta(\infty)N'_{\text{tot}}\sum_q k_q(qV_{\text{front}})F_q(\infty). \end{aligned} \tag{3}$$

In principle we could measure N_{counted} at any energy, but by selecting data at the highest values of V_{front} possible, the values of k_q and, hence, the corrections to N_{counted} and R_c are minimized. Note that as a function of charge state, i.e., impact energy, $k_q<1$ and increases in magnitude with increasing q. $F_q(\infty)$ is also less than 1 but for electron impact quickly decreases in magnitude with increasing q. As a function of ion mass, i.e., impact velocity, both k_q and $F_1(\infty) \rightarrow 1$ for light ions and decrease in magnitude for heavier ions. This means that the summation in Eq. (3), which is the correction to N_{counted}, increases in magnitude with increasing ion mass. Equation (3) also shows that the number of ions counted is less than the number that arrive at the detector, e.g., $N_{\text{counted}}<\mathrm{N}'_{\text{tot}}$.

In contrast, our "current mode" technique measures total charge arriving at the detector. This means that multiply charged ions are overcounted and different corrections are

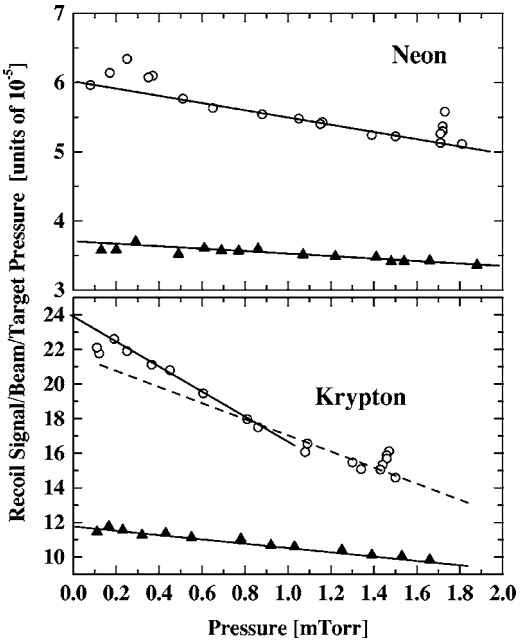

FIG. 2. Recoil ion signal per incident beam intensity and target pressure as a function of target gas pressure. Ratios are for the number of recoil ions counted (closed symbols) and for the recoil ion current (open symbols). The lines are eyeball fits to the data.

needed to convert the measured current into the total number of particles. The total ion current, I_{tot} is given by

$$I_{\text{tot}} = \sum_q I_q = \sum_q qeN'_q = eN'_{\text{tot}} \sum_q qF_q(\infty). \tag{4}$$

Here, e is the electron charge, q is the ion charge state, and the other values have already been defined.

Dividing Eq. (3) by the integrated beam intensity and Eq. (4) by the beam current converts the left-hand sides of Eqs. (3) and (4) to the ratios R_c and R_I. Then dividing Eq. (3) by Eq. (4) shows that the absolute asymptotic detection efficiency $\eta(\infty)$ can be determined from

$$\eta(\infty) = \frac{N_{\text{counted}}}{I_{\text{tot}}/e} \frac{\sum_q qF_q(\infty)}{\sum_q k_q(qV_{\text{front}})F_q(\infty)} = \frac{R_c}{R_I} \frac{\sum_q qF_q(\infty)}{\sum_q k_q(qV_{\text{front}})F_q(\infty)}. \tag{5}$$

Equation (5) demonstrates that the absolute detection efficiency can be determined from our ion counting and current ratio measurements, plus sums over $F_q(\infty)$ (from our step 1 TOF measurements) and over $k_q(qV_{\text{front}})$ (from our step 2 relative counts versus the impact energy curve).

In Fig. 2, we compare the ratios R_c and R_I where both have been divided by the target pressure. As seen, both R_c/P and R_I/P vary with target pressure and for heavy targets R_I/P always demonstrated a change in slope in the vicinity of 1 mTorr. These features are not understood but were always present. In evaluating Eq. (5) both curves were extrapolated to zero target pressure, as indicated by the solid lines in Fig. 2. This provided values for $\eta(\infty)$ for each target gas and by normalizing the relative counts versus impact energy curves to these values absolute detection efficiencies for energies ranging from approximately 0.25 to 25 keV were obtained.

III. RESULTS AND DISCUSSION

Table I lists the values for $\eta(\infty)$ obtained for each gas, plus an average for all gases. Data are for a channelplate and for two channel electron multipliers. On average, the asymptotic efficiency for the CP was approximately 58% whereas for both CEMs it was roughly 89%. Standard deviations in both cases are approximately ±10%. Experimental uncertainties for various parameters which contribute to the uncertainties in the individual efficiency measurements include (i) R_c, 0.5%–10% (arising from the pressure readings); (ii) R_I, 1%–2% (accuracy of reading I_{tot}); (iii) the ratio R_c/R_I, 5%–10% (from measured reproducibilities, extrapolation to zero pressure, and errors in measuring R_c and R_I); (iv) $N_{\text{tot}}(V_{\text{front}})$, 1%–4% (due to a systematic underestimation of beam current because of electrometer zero adjustments; it is largest for the heaviest gases because the currents were smallest); (v) $\Sigma\, qF_q$, <2% (dominated by the uncertainty in F_1); (vi) $\Sigma\, k_qF_q$, <5% (dominated by uncertainties in the $q=1,2$ terms); all other contributions being small. Combining the above uncertainties that contribute directly to $\eta(\infty)$ gives a total expected uncertainty of −10% to +14% which is consistent with the scatter seen for the different gases.

With regard to the absolute detection efficiencies for different ions, as mentioned it might be expected that the efficiency depends only on the particle's impact energy or velocity. But, for the ions investigated in this work we found neither of these scalings to be appropriate. For a channelplate, we found that plotting the efficiencies versus the impact energy divided by the square root of the ion mass, $E/M^{0.5}$ compressed the data for various ions into a single

TABLE I. Values for $\eta(\infty)$ measured for a channelplate and two CEMs. All values are in percent. Where repeat measurements were made, both values are listed.

Detector	N^+, N_2^+	O^+, O_2^+	Ne^{q+}	Ar^{q+}	Kr^{q+}	Xe^{q+}	Average
Channelplate	56.2		62.5	69.7	51.8	48.7	57.8±8.4
CEM 1 (new)	86.1	94.5	105.9	89.6	87.8	84.2	89.3±8.0
		86.1		92.0	77.1		
CEM 2 (used)	89.4	113.0	86.5	74.0	72.0	79.3	88.2±13.5
			94.0			79.4	

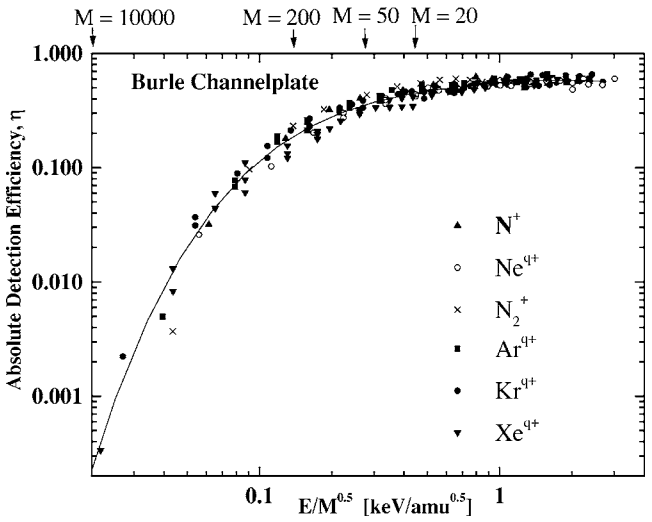

FIG. 3. Absolute ion detection efficiencies for a channelplate. The efficiencies are plotted vs the impact energy divided by the square root of the ion mass. The solid line is a polynomial fit to all the data. Arrows on the top axis indicate values of the abscissa for detecting singly charged positive ions of various masses if the front plate is biased at −2 kV and the backplate of a chevron pair is grounded as is often used for channelplate pairs.

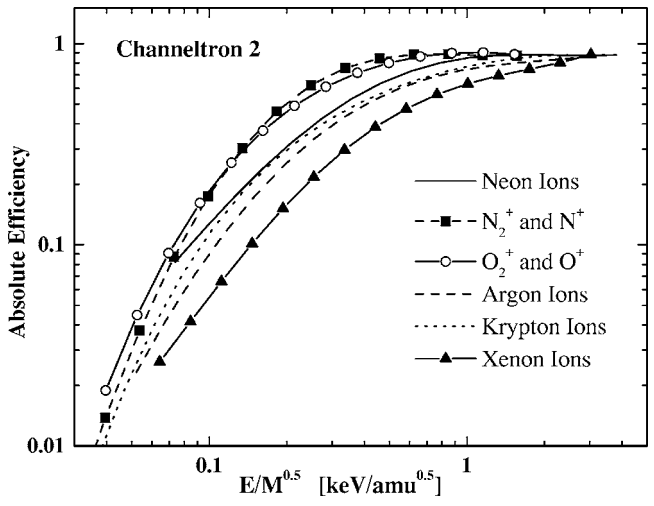

FIG. 4. Ion detection efficiencies measured for CEM 2. Lines and lines with symbols representing polynomial fits to the data for each ion species are shown rather than individual data points.

curve, as shown in Fig. 3. (While drafting this manuscript we became aware of the work of Burrous *et al.*[19] who arrived at a similar scaling, e.g., a $vA^{0.4}$ scaling, where v and A are the ion velocity and atomic number.) The solid line is a polynomial fit to all the data in Fig. 3 with the fitting parameters listed in Table II. Also given in Table II are the charge states used for each ion.

Also included in Fig. 3 are arrows indicating scaled energies for detecting various singly charged positive ions under "normal" operating conditions. By normal operating conditions, we mean biasing the front plate of a chevron pair at the full operating voltage of −2 kV and grounding the backplate. Note that only above a scaled energy of 1 is the efficiency nearly constant. Using a 2 kV bias voltage, this corresponds to ions of mass 4 or smaller. In studies using heavier ions where different masses or different charge states of the same ion are detected, the detection efficiencies can be quite different for each particular ion. In particular, note that if these results are extrapolated to very heavy ions such as fullerenes or extremely large biological species the detection efficiencies will only be a few percent or smaller unless the ions are preaccelerated to many keV. For comparison purposes the only efficiency for very heavy ions that we are aware of is the value of 5% for 30 keV mass 66400 amu ions.[20] Our data in Fig. 3 predicts an efficiency that is slightly larger than 10%.

Applying the same scaling procedure to our CEM data shifts the neon, argon and krypton data to nearly a common curve but, as seen in Fig. 4, this curve lies between the molecular nitrogen and oxygen data and the xenon data. We found that $E/M^{0.6}$ gave a slightly better compression but still no single curve emerged. Thus, polynomial fits were made to the measured CEM efficiencies plotted versus the impact energies in keV. Table II provides these parameters for both CEMs and for all ions investigated.

TABLE II. Fitting parameters for polynomials fitted to the measured efficiency data. The polynomial is given by $\log[\eta]=A+Bx+Cx^2+Dx^3+Fx^4$ with x as indicated in the table. The impact energy E is in keV and the ion mass M is in amu. For the channelplate, the fit is to the single scaled set of data. For the CEMs, the efficiencies vs impact energy were fitted for each set of ions investigated.

Detector	A	B	C	D	F	x
Channelplate all gases	−0.257	0.161	−0.239	−0.0184	−0.300	$\log[E/M^{0.5}]$
CEM 1						log[E]
Ne^{q+}(q=1−3)	−0.479	1.198	−0.970	0.160	0.046	
O_2^+	−0.414	1.329	−1.868	1.245	−0.303	
Kr^{q+}(q=1−5)	−1.012	1.962	−2.098	1.476	−0.450	
Xe^{q+}(q=1−5)	−1.313	2.144	−1.763	1.264	−0.461	
CEM 2						log[E]
Ne^{q+}(q=1−3)	−0.459	1.051	−0.659	−0.198	0.208	
N_2^+	−0.320	1.127	−1.450	0.438	0.155	
O_2^+	−0.389	1.059	−1.115	0.542	−0.159	
Ar^{q+}(q=1−4)	−0.725	1.410	−0.957	0.091	0.087	
Kr^{q+}(q=1−5)	−0.879	1.667	−1.418	0.686	−0.160	
Xe^{q+}(q=1−5)	−1.360	1.677	−0.120	−0.701	0.279	

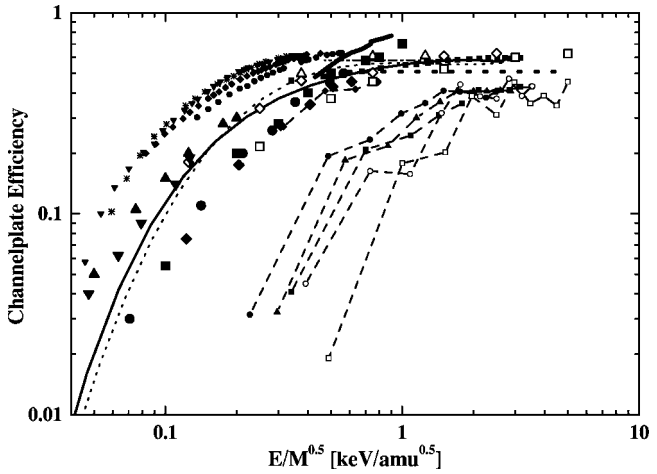

FIG. 5. Comparison of channelplate efficiencies measured in this work (solid curve) with previous measurements. Dotted curve, from Ref. 7; small solid symbols ■,●,◆,*,▼ for H_2^+,Ne^+,Ar^+,Kr^+,Xe^+, from Ref. 9; large symbols □,◇,◆,△ for H^+,He^+,He^0, and O^+, from Ref. 2; horizontal dot-dash curve, 5.4 keV He^+,C^+,O^+,N_2^+,CO^+,CO_2^+,SO_2^+, Kr^+, and Xe^+, from Ref. 10; horizontal dashed curve, 1–10 keV He and He^+, from Ref. 5; broad solid line, Mg^+, from Ref. 3; dashed curves with symbols, ■,●,▲,□,○,◆ for H_2^+, D_2^+, HD^+, H^+, D^+, Ar^+, from Ref. 8; H^+, D^+, O^+, and Ar^+, large solid symbols ■,●,▲,▼, from Ref. 13; large solid diamond, Na^0 and Na^+ data from Ref. 14.

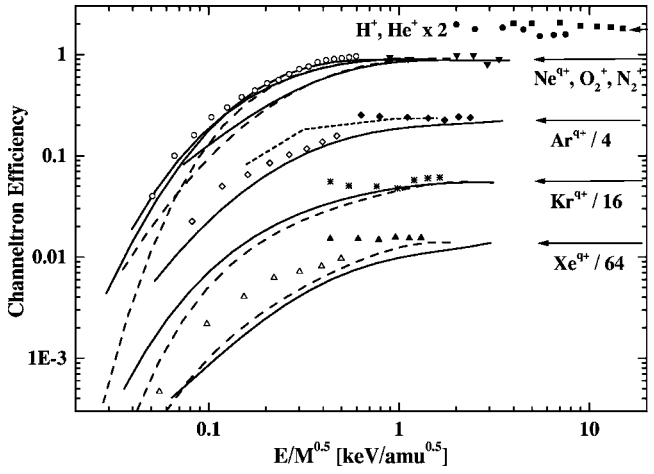

FIG. 6. Comparison of measured CEM efficiencies. Solid and dashed curves, present work for CEM 1 and 2, respectively; solid symbols, ■,●,▼,◆,*,▲ for H^+, He^+, Ne^+, Ar^+, Kr^+, Xe^+ from Ref. 1; open symbols, ○, ◇, △ for He^+, Ar^+, Xe^+ from Ref. 12; dotted curve for Ar^+ from Ref. 11. The various datasets have been displaced vertically as indicated for display purposes. The arrows on the right indicate the same, but shifted, asymptotic values for the efficiency.

A comparison of the present channelplate efficiencies with previous work is shown in Fig. 5. Here, the solid curve is the polynomial fit taken from Fig. 3. It is seen to be in good agreement with results obtained using a different procedure reported previously by one of the authors.[7] Comparing the present results with previously reported data show the following. There is good agreement, particularly at high energies, with the measurements of Gao *et al.*[2] and Straub *et al.*[10] and, within error bars, of those of Tobita *et al.*[5] In contrast, the present data are smaller than those of Oberheide *et al.*[9] except for the case of H_2^+ where the agreement is nearly perfect, and they are larger than those of Brehm *et al.*[8] The low-energy O^+ and Ar^+ data of Peko and Stephen[13] show similar trends with the present results and quite good agreement at their highest energy. It is important to keep in mind that some of the differences noted here, particularly at lower impact energies, may be attributed to the presence or absence of electric fields used by different researchers to suppress the loss of secondary electrons from the surface of the channelplate.

Figure 5 also demonstrates that "lighter" ions tend to behave differently from "heavier" ions. Although the available light ion data provide mixed messages, it is interesting to note that the H^+ data of Gao *et al.*,[2] the H^+ and D^+ data of Peko and Stephen[13] and the Na^0 and Na^+ data of Barat *et al.*[14] all scale to a single curve but this curve is different from the one that the heavier ion data scale to. This effect was also found to be present in the relative efficiency measurements of Yagi *et al.*[15] (not shown). However, other light ion data, i.e., the H_2^+ data of Oberheide *et al.* and the He^+ data of Gao *et al.*, are in better agreement with the "heavy" ion data. Obviously, additional measurements are needed in order to investigate this. However, whether for light or heavy ions the majority of the data indicate that the maximum channelplate efficiency is between 55% and 65%, in contradiction with the measurements of Müller *et al.*[3]

In Fig. 6 the present CEM efficiencies are compared with previous measurements. For display purposes, the various datasets have been shifted vertically. The solid and dashed curves are for the two CEMs we investigated. Except at lower energies where the observed differences are possibly attributed to different ion energies, within error bars we find no difference between the two CEMs, i.e., no difference due to manufacturer or usage. (The reader is reminded that the impact energy depends on where and, hence, at what potential, the ions impact on the CEM cone.) At high energies, the present data are in excellent agreement with the measurements of Fricke *et al.*[1] although the present work clearly indicates an energy dependent efficiency whereas the work of Fricke *et al.* does not. Our energy dependence is confirmed by the work of Tassoto and Watson.[12] Finally, note that our work plus the work of Fricke *et al.* agree that the maximum CEM efficiency is approximately 90%.

IV. CONCLUDING REMARKS

One important point of this work is that a channel electron multiplier has a maximum efficiency for detecting positive ions of approximately 89%. For a channelplate the maximum efficiency is approximately 58% which is slightly larger than the open aperture ratio (as might be expected if all ions entering the channels are detected) and considerably larger than what would be expected from multiplying the CEM efficiency by the CP open aperture ratio. A second important finding is that for the ions investigated, neon to xenon, the detection efficiencies are not simply a function of the impact velocity or the impact energy. Rather, for a channelplate the efficiencies scale to a single curve when plotted as a function of the impact energy divided by the square root of the ion mass. For a CEM this scaling worked only for a

limited subset of ions. In contrast, data taken from the literature indicate that the detection efficiencies for light ions scale differently.

Finally, the good agreement between our present channelplate efficiencies and those in Ref. 7 implies that the channelplate efficiencies reported here are applicable for any channelplate detector array, at least for the ion mass range investigated and possibly for much heavier species as well. In addition, the CEM efficiencies indicate that our results should apply to any CEM detector if the impact energies are sufficiently large in order to neglect uncertainties associated with the exact cone potential. Hence, where absolute or relative detection efficiencies are required, they can be directly obtained using information provided in Table II or the user could perform his own time-of-flight and total number of detected ion measurements as described above, then use Eq. (1) to generate $N_q(E_q)$ data for his specific detector and normalize these data to the $\eta(\infty)$ values listed in Table I.

ACKNOWLEDGMENTS

This work supported in part by the National Science Foundation and the Office of Fusion Energy Sciences at the Department of Energy.

[1] J. Fricke, A. Müller, and E. Salzborn, Nucl. Instrum. Methods **175**, 379 (1980).
[2] R. S. Gao, P. S. Gibner, J. H. Newman, K. A. Smith, and R. F. Stebbings, Rev. Sci. Instrum. **55**, 1756 (1984).
[3] A. Müller, N. Djurić, G. H. Dunn, and D. S. Belić, Rev. Sci. Instrum. **57**, 349 (1986).
[4] T. Sakurai and T. Hashizume, Rev. Sci. Instrum. **57**, 236 (1986).
[5] K. Tobita, H. Takeuchi, H. Kimura, Y. Kusama, and M. Nemoto, Jpn. J. Appl. Phys., Part 1 **26**, 509 (1987).
[6] R. D. DuBois, Phys. Rev. A **36**, 2585 (1987).
[7] R. D. DuBois and A. Kövèr, Phys. Rev. A **40**, 3605 (1989).
[8] B. Brehm, J. Grosser, T. Ruscheinski, and M. Zimmer, Meas. Sci. Technol. **6**, 953 (1995).
[9] J. Oberheide, P. Wilhelms, and M. Zimmer, Meas. Sci. Technol. **8**, 351 (1997).
[10] H. C. Straub, M. A. Mangan, B. G. Lindsay, K. A. Smith, and R. F. Stebbings, Rev. Sci. Instrum. **70**, 4238 (1999).
[11] S. Shchemelinin, S. Pszona, G. Garty, A. Breskin, and R. Chechik, Nucl. Instrum. Methods Phys. Res. A **438**, 447 (1999).
[12] M. Tassoto and P. R. Watson Rev. Sci. Instrum. **71**, 2704 (2000).
[13] B. L. Peko and T. M. Stephen, Nucl. Instrum. Methods Phys. Res. B **171**, 597 (2000).
[14] M. Barat, J. C. Brenot, J. A. Fayeton, and Y. J. Picard, Rev. Sci. Instrum. **71**, 2050 (2000).
[15] S. Yagi, T. Nagata, M. Koide, Y. Itoh, T. Koizumi, and Y. Azuma, Nucl. Instrum. Methods Phys. Res. B **183**, 476 (2001).
[16] E. S. Parilis and L. M. Kishinevskii, Sov. Phys. Solid State **3**, 885 (1960).
[17] G. W. Fraser, Int. J. Mass. Spectrom. **215**, 13 (2002).
[18] B. Deconihout, F. Vurpillot, M. Bouet, and L. Renaud, Rev. Sci. Instrum. **73**, 1734 (2002).
[19] C. N. Burrous, A. J. Leiber, and V. T. Zaviantseff, Rev. Sci. Instrum. **38**, 1477 (1967).
[20] M. Frank, Nucl. Instrum. Methods Phys. Res. A **444**, 275 (2000).